

Finite elements of mixed interface for models of cohesive zone (**xxx_INTERFACE** and **xxx_INTERFACE_S**)

Summary:

This document presents a finite element of mixed interface for models of cohesive zone. Keywords corresponding for modelings in *Code_Aster* are `PLAN_INTERFACE`, `AXIS_INTERFACE`, `3D_INTERFACE`, `PLAN_INTERFACE_S`, `AXIS_INTERFACE_S` and `3D_INTERFACE_S`.

Contents

1 Introduction.....	3
2 Construction of the finite element of mixed interface.....	3
2.1 Principle of minimization of energy in breaking process.....	3
2.2 Search for point saddles by a method of decomposition – coordination.....	3
2.2.1 Lagrangian increased.....	4
2.2.2 Characterization of the point saddles.....	4
2.3 Discretization of the finite element.....	4
3 Integration of the cohesive law CZM_TAC_MIX.....	7
3.1 Preliminary notations.....	7
3.2 Definition of the cohesive law.....	7
3.3 Digital integration.....	10
4 Conclusion.....	13
5 Bibliography.....	14
6 Description of the versions of the document.....	14

1 Introduction

This model of cohesive zone gives an account of the phenomena of starting of crack, propagation (in a given direction) and of final rupture. The mixed element of interface is introduced to discretize the way of cracking of which the degrees of freedom are the displacement of the two lips of the crack, as well as the density of the cohesive forces. The construction of the model of finite element and the integration of the constitutive law `CZM_TAC_MIX` are detailed. This document is largely inspired by the Lorentz article 5, the interested reader can refer to it for more details.

2 Construction of the finite element of mixed interface

2.1 Principle of minimization of energy in breaking process

In their approach of the breaking process, Frankfurt and Marigo 5 describe the state of a structure Ω by a field of displacement u being able to admit discontinuities $\delta = [[u]]$ through surfaces $\Gamma(u)$. For a loading given displacement is characterized by a condition of optimality: it corresponds at least local of definite potential energy as the sum of the elastic deformation energy, cohesive energy and the work of the external forces:

$$E_{\text{pot}}(u) = E_{\text{el}}(u) + E_{\text{fr}}([[u]]) - W_{\text{ext}}(u)$$
$$E_{\text{el}}(u) = \int_{\Omega \setminus \Gamma(u)} \Phi(\varepsilon(u)) d\Omega ; E_{\text{fr}}(\delta) = \int_{\Gamma(u)} \Pi(\delta) dS$$

where ε indicate the tensor of the deformations, Φ density of deformation energy (voluminal) and Π density of cohesive energy (surface). In this formulation, the mechanisms of rupture are regarded as reversible. The irreversibility will be introduced into the following part, starting from internal variables. The characteristics of the problem are deduced from minimization, namely:

- the forecast of the way of cracking, since one takes into account all possible discontinuous displacements;
- a criterion in constraint for the crack initiation (see 5).
- the cohesive law connects the discontinuity of displacement δ with the vector of traction t starting from the derivative (generalized) of Π ;
- the conditions of contact, are managed via the cohesive energy to which one adds a function of indicatrix prohibiting the interpenetration of the lips.

However, to take account of all possible discontinuous displacements involves digital difficulties related to the discretization of functional space $BD(\Omega)$. In particular, to authorize discontinuities through each finite element leads to a dependence of the results to the grid. Alternative works are completed, based on the regularization of discontinuities 5 or on the adaptation of the grid 5. The latter are however limited to energies of surface of the type Griffith (without cohesive forces) and lead to important digital difficulties. This is why we introduce a simplification into our model by considering that surfaces potential discontinuities of displacement Γ are applied *a priori* and that they do not depend any more u .

2.2 Search for point saddles by a method of decomposition – coordination

In spite of the postulate on the direction of cracking, the minimization of energy is not obvious taking into account the non-derivability of the energy of surface. One bases oneself here on the technique of decomposition – coordination introduced into 5, which condenses the non-derivability on a local level (points of Gauss).

2.2.1 Lagrangian increased

The relation between the field of discontinuity δ and the field of displacement u is introduced explicitly into minimization, total energy E thus depends explicitly on u and of δ :

$$E(u, \delta) = \int_{\Omega \setminus \Gamma} \Phi(\varepsilon(u)) d\Omega - W_{ext}(u) + \int_{\Gamma} \Pi(\delta) d\Gamma$$

The minimization of the potential energy is then equivalent to the problem of minimization under constraint according to (displacement pertaining to the whole of displacements kinematically acceptable):

$$\min_{\substack{u, \delta \\ [[u]] = \delta}} E(u, \delta)$$

The linear constraint $[[u]] = \delta$ is treated by dualisation : a solution (u, δ) of corresponds to a point saddles (u, δ, λ) Lagrangian following, where λ corresponds to the field of the multipliers of Lagrange:

$$\mathbf{L}(u, \delta, \lambda) \stackrel{def}{=} E(u, \delta) + \int_{\Gamma} \lambda \cdot ([[u]] - \delta) d\Gamma$$

Lastly, to gain in coercivity compared to δ , which will prove to be necessary thereafter, one adds a quadratic term of penalization not having no influence on the solution since it is equal to zero when the constraint is checked. The Lagrangian one increased \mathbf{L}_r , with the coefficient of penalization r is written then:

$$\mathbf{L}_r(u, \delta, \lambda) \stackrel{def}{=} E(u, \delta) + \int_{\Gamma} \lambda \cdot ([[u]] - \delta) d\Gamma + \int_{\Gamma} \frac{r}{2} ([[u]] - \delta)^2 d\Gamma$$

2.2.2 Characterization of the point saddles

The conditions of optimality of a nature 1 for the Lagrangian one increased, are written in the following way:

$$\begin{aligned} \forall \delta \int_{\Gamma} [t - \lambda - r ([[u]] - \delta)] \cdot \delta d\Gamma &= 0 \quad \text{avec } t \in \partial \Pi(\delta) \\ \forall \delta u \int_{\Omega \setminus \Gamma} \sigma : \varepsilon(\delta u) + \int_{\Gamma} [\lambda + r ([[u]] - \delta)] \cdot [[\delta u]] &= W_{ext}(\delta u) \quad \text{avec } \sigma = \frac{\partial \Phi}{\partial \varepsilon}(\varepsilon) \\ \forall \delta \lambda \int_{\Gamma} ([[u]] - \delta) \cdot \delta d\Gamma &= 0 \end{aligned}$$

Significance of the under-differential $\partial \Pi$ is given in the part 3. This stage, one is satisfied to say that $t \in \partial \Pi(\delta)$ mean that t and δ are connected by the cohesive law. The equation thus give an interpretation of the multiplier of Lagrange λ : except the term of penalization, it is the cohesive forces. The equation express the balance of the efforts in the volume and along the surface of discontinuity Γ . Lastly, impose the constraint between the field of displacement and its discontinuities.

2.3 Discretization of the finite element

Since the trajectory of the crack Γ is defined *a priori* and thanks to the assumption of the small disturbances, the space discretization of the system - can be pressed on a finite element of interface. Let us suppose that the under-fields Ω_- and Ω_+ (parts of Ω respectively in lower part and with the top of Γ) are discretized by tetrahedrons or hexahedrons so that the nodes on each side of Γ coincide¹. In this case, degenerated prisms or hexahedrons can be used to discretize Γ and to connect the two lips Γ_- and Γ_+ potential cohesive crack (see Figure 2.3-a).

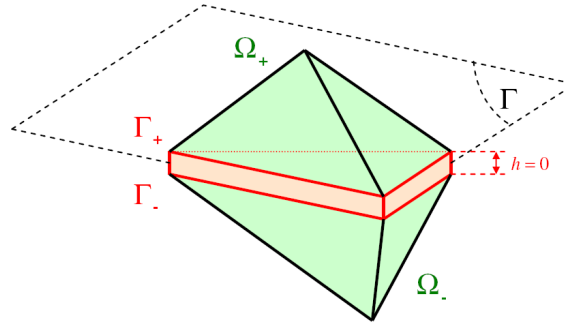


Figure 2.3-a : Discretization by finite element of interface.

That is to say a grid characterized by the parameter h (for example, maximum size of the finite elements). In the field Ω one adopts a quadratic interpolation with finite elements of Lagrange classics (P2-continuous). The space discretized of **fields of displacements** U_h is written:

$$U_h = \{ u ; \forall x \in \Omega \ u(x) = [N(x)] \{ U \} \}$$

where $\{ U \}$ indicate the vector of nodal displacements and $[N]$ the matrix of the quadratic functions of forms. The trace of the displacement interpolated on Γ_- and Γ_+ is also quadratic per pieces and the discontinuity of displacement is expressed in the following way:

$$\begin{aligned} \forall x \in \Gamma \ u|_{\Gamma_-}(x) &= [N_-(x)] \{ U \} ; \ u|_{\Gamma_+}(x) = [N_+(x)] \{ U \} \\ \forall x \in \Gamma \ \llbracket u(x) \rrbracket &= [D(x)] \{ U \} \quad \text{avec} \quad [D(x)] = \underset{\text{d\'ef.}}{[N_+(x)] - [N_-(x)]} \end{aligned}$$

where $[N_-]$ and $[N_+]$ correspond respectively to the trace of $[N]$ on Γ_- and Γ_+ and where $[D]$ indicate the matrix of the functions of the quadratic forms which interpolates the jump of displacement. Let us note that it can be useful to introduce a rotation into $[D]$ in order to obtain the components of $\llbracket u \rrbracket$ in a local frame of reference and to distinguish the normal and tangential parts thus.

field of the multipliers of Lagrange λ is interpolated on Γ by linear functions of forms per pieces (P1-continuous), leading to space discretized of the multipliers of Lagrange L_h according to:

$$L_h = \{ \lambda ; \forall x \in \Gamma \ \lambda(x) = [L(x)] \{ A \} \}$$

where $\{ A \}$ corresponds to the nodal unknown factors of the multiplier of Lagrange and $[L]$ indicate the matrix of the linear functions of forms on Γ . In this way, the constraint $\llbracket u \rrbracket = \delta$ imposed by is realized only with the weak direction.

¹ That does not pose a priori a problem with the algorithms of grid, at least for the cracks having a simple form, for example plane.

To finish, discretization of **field of discontinuity** $\delta \in D_h$ is based on the points of collocation on Γ , coordinates x_g . These points correspond to the points of Gauss, of weight ω_g , used to calculate the integrals. Here a standard modeling, and a modeling known as under-integrated are distinguished.

- In standard modeling, the points of Gauss are 3 (segments), 6 (triangles) or 9 (quadrilaterals) per element. This corresponds to an interpolation P2-discontinuous of δ . This choice has the advantage of limiting the risk of appearance of worthless pivots in the tangent matrix, but it does not check condition LBB within the limit of a parameter of penalization r infinite.
- In under-integrated modeling, the points of Gauss are 2 (segments), 3 (triangles) or 4 (quadrilaterals) per element. This corresponds to an interpolation P1-discontinuous of δ . This choice checks best condition LBB within the limit $r \rightarrow \infty$, but it is likely to reveal worthless pivots in the tangent matrix. These worthless pivots appear when the rigidity of the elements in contact with the interface is not enough to ensure coercivity of the formulation, in particular when the interface is on a symmetry plane, or between a volume and an element of structure (bars, grid or membrane).

The space discretization, the notations as well as the diagrams of the finite elements for under-integrated modeling are summarized on Figure 2.3-b.

Field	Shape functions	Unknowns	Interpolation	Finite element
displacement $\mathbf{u} \in \mathcal{W}_h$	cont-P2 $[\mathbf{N}(\mathbf{x})]$	nodal $\{\mathbf{U}\}$	$\mathbf{u}(\mathbf{x}) = [\mathbf{N}(\mathbf{x})]\{\mathbf{U}\}$	
displ. discontinuity $[\mathbf{u}]$	cont-P2 $[\mathbf{D}(\mathbf{s})]$	nodal $\{\mathbf{U}\}$	$[\mathbf{u}](\mathbf{s}) = [\mathbf{D}(\mathbf{s})]\{\mathbf{U}\}$	
Lagrange mult. $\lambda \in \mathcal{L}_h$	cont-P1 $[\mathbf{L}(\mathbf{s})]$	nodal $\{\Lambda\}$	$\lambda(\mathbf{s}) = [\mathbf{L}(\mathbf{s})]\{\Lambda\}$	
displ. discontinuity $\delta \in \mathcal{D}_h$	disc-P1	Gauss points δ_g	$\delta(\mathbf{s}_g) = \delta_g$	

Figure 2.3-b : Space discretization

The field δ disappears from the total formulation thanks to static condensation. Indeed, with the adopted discretization, the resolution of δ come down to satisfy the cohesive law in each point with collocation:

$$t_g = \lambda_g + r \left(\left[[u_g] \right] - \delta_g \right) \in \partial \Pi(\delta_g) \quad \text{avec} \quad \begin{cases} \left[[u_g] \right] = [D_g][U] & ; \quad [D_g] = [D(x_g)] \\ \mu_g = [L_g][A] & ; \quad [L_g] = [L(x_g)] \end{cases}$$

The integration of the constitutive relation (i.e the resolution of, cf left following), makes it possible to calculate δ_g function of $[U]$ and $[A]$ that one notes δ :

$$t_g = \lambda_g + r \left(\left[[u_g] \right] - \delta_g \right) \in \partial \Pi(\delta_g) \quad \Leftrightarrow \quad \delta_g = \hat{\delta} \left(\left[[u_g] \right], \lambda_g \right) = \delta(U, A)$$

The parameter of penalization r allows to ensure the unicity of whatever $[U]$ and $[A]$ (cf left following). That constitutes a requirement to guarantee robustness of the model.

There is then the nonlinear system whose unknown factors are nodal displacements $[U]$ and the nodal multiplier of Lagrange $[A]$:

$$\int_{\Omega \setminus \Gamma} [\nabla N]^T : \boldsymbol{\sigma}(U) + \sum_g \omega_g [D_g]^T \cdot ([L_g][A] + r[D_g][U] - r \delta(U, A)) = \{F_{\text{ext}}\}$$

$$\sum_g \omega_g [L_g]^T \cdot ([D_g][U] - \delta(U, A)) = 0$$

The integral of volume and the nodal vector of the external efforts are calculated in a usual way. Lastly, the system is solved simultaneously compared to $\{U\}$ and $\{A\}$ by means of a method of Newton (generalized), where the tangent operator is symmetrical since - corresponds to a search for point saddles.

3 Integration of the cohesive law CZM_TAC_MIX

The cohesive behavior is determined by the density of cohesive energy $\Pi(\delta)$. Although the variational formulation presented in the preceding part is independent of the choice of cohesive energy, we are interested now in a particular cohesive model which one details specificities. These main features are:

- conditions of contact (not interpenetration of the lips);
- perfect initial adherence (not of regularization of the energy of surface);
- coupling between the modes of rupture (traction and shearing);
- total rupture, (worthless cohesive forces beyond of a certain threshold of damage);
- irreversibility of the rupture.

That means in particular that there is no final friction, nor distinction between the mechanisms of rupture in traction and shearing.

Notice :

The Code_Aster keyword corresponding to this cohesive law is `CZM_TAC_MIX`. For more details on this law (internal variables, parameters of entry, coherent tangent matrix) and on other cohesive laws, one can refer to 5 (R7.02.11).

3.1 Preliminary notations

Because of the constraint of noninterpenetration of the lips of the crack, the direction n normal for the surface of potential discontinuity Γ (opening/compression) must be distinguished from the directions in the plan (slip, shearing). With this intention, the following notations are introduced, where v represent any vector quantity:

$$v_n = v \cdot n \quad ; \quad v_{//} = v - v_n n \quad ; \quad \langle v \rangle_+ = \langle v_n \rangle n + v_{//} \quad ; \quad \|v\|_+ = (\langle v \rangle_+ \cdot \langle v \rangle_+)^{1/2}$$

and where $\langle \cdot \rangle$ indicate the positive part of a scalar.

3.2 Definition of the cohesive law

The cohesive law suggested by Heel and Curnier 5 answers the five points mentioned previously and returns within the framework of the energy formulation. Answers of the model subjected to a pure traction and a pure shearing, as well as the criterion of starting in constraint are detailed Figure 3.2-a .

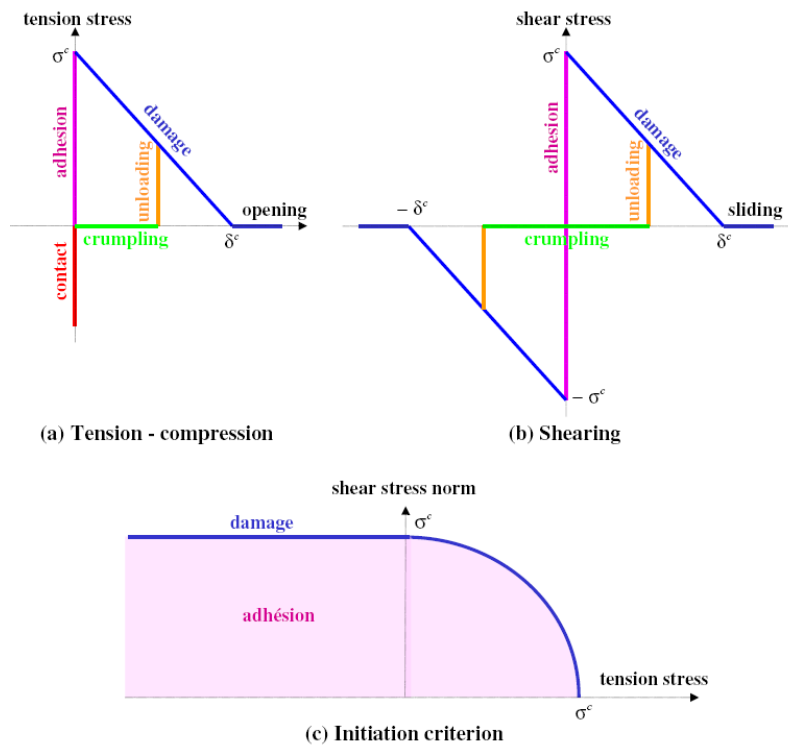


Figure 3.2-a : Answers of the law Talon Curnier CZM_TAC_MIX in pure traction and compression (A), pure shearing (b) and criterion of starting in constraint (c)

Corresponding cohesive energy is defined as follows:

First of all, discontinuities of displacement in opening and shearing are gathered in a single scalar δ_{eq} who measures the amplitude of discontinuity, thus answering the point 3 :

$$\delta_{eq} = N(\delta) = \sqrt{\delta \cdot \delta}$$

Then, account of the irreversibility is taken 3 via a new variable interns scalar κ who measures the maximum level of loading running:

$$\kappa(t) = \max_{t' < t} \delta_{eq}(t')$$

Cohesive energy depends on the internal variable κ and of the jump of displacement are equivalent δ_{eq} . Conditions of contact 3 are managed by an indicating function which imposes a positive normal discontinuity $\delta_n \geq 0$:

$$\Pi(\delta, \kappa) = I_{\mathbb{R}^+}(\delta_n) + \psi(\max(\delta_{eq}, \kappa))$$

The function ψ characterize in particular the reaction to a request in mode I pure. According to 5, ψ must be an increasing and derivable function, where $\sigma^c = \psi'(0)$ defines the critical stress, parameter of the criterion of starting 3 represented on Figure 3.2-a. In addition, the stability of the process of rupture requires that ψ that is to say concave 5. Lastly, final rupture 3 occurs as soon as ψ reached its higher limit G^c for a finished value $\delta_{eq} = \delta^c$, where G^c is the energy of rupture and δ^c the critical opening beyond which the cohesive forces are cancelled.

Thus, the function is chosen ψ following which corresponds to the answers represented on Figure 3.2-a :

$$\psi(\delta_{eq}) = \begin{cases} G^c \frac{\delta_{eq}}{\delta^c} \left(2 - \frac{\delta_{eq}}{\delta^c} \right) & \text{if } \delta_{eq} \leq \delta^c \\ G^c & \text{if } \delta_{eq} \geq \delta^c \end{cases}$$

with the relation between the parameters materials;

$$G^c = \frac{1}{2} \sigma^c \delta^c$$

This stage, the energy and the cohesive law which in drift are entirely defined. However, one can explicitly express the relation between the discontinuity of displacement δ and the vector forced t , in a way condensed in following differential inclusion, where $\partial \Pi$ is the under-differential of Π (see Clarke 5):

$$t \in \partial \Pi(\delta)$$

For a value given of κ , one can interpret the under-differential $\partial \Pi(\delta)$ like the cone formed by the whole of the directional slopes of the derivative of Π in δ for all the acceptable directions. Mathematically, that is formulated in the following way:

$$\partial \Pi(\delta) = \left\{ t \in R^3 ; \forall v \in R^3 \quad t \cdot v \leq \Pi^\circ(\delta, v) \right\}$$

where $\Pi^\circ(\delta, v)$ is the directional derivative of Π compared to δ in direction v :

$$\Pi^\circ(\delta, v) = \limsup_{\substack{\rho \rightarrow 0^+ \\ d \rightarrow \delta}} \frac{\Pi(d + \rho v) - \Pi(d)}{\rho}$$

This definition coincides with the gradient of Π everywhere where this one is derivable. According to the definition, the points deserving a special attention are $\delta = 0$, $\delta_n = 0$ and $\delta_{eq} = \kappa$. One thus deduces from the four following cases (magazines color on Figure 3.2-a):

- 1) Not ($\kappa = 0$ and $\delta = 0$): perfect adherence, i.e criterion of starting (connects pink)

$$\partial \Pi(\delta) = \left\{ t \in R^3 ; \|t\|_+ \leq \sigma^c \right\}$$

- 2) Field where $\delta_{eq} < \kappa$: return to zero with worthless constraint (connects green)

$$\partial \Pi(\delta) = \left\{ t_n n ; t_n \leq 0 \text{ et } \delta_n \geq 0 \text{ et } t_n \delta_n = 0 \right\}$$

- 3) Very cone $\delta_{eq} = \kappa > 0$: vertical discharge of the constraint (connects orange)

$$\partial \Pi(\delta) = \left\{ t_n n + \rho \delta ; 0 \leq \rho \leq \frac{\psi'(\kappa)}{\kappa} \text{ et } t_n \leq 0 \text{ et } \delta_n \geq 0 \text{ et } t_n \delta_n = 0 \right\}$$

- 4) Field where $\delta_{eq} > \kappa$: damage (connects blue)

$$\partial \Pi(\delta) = \left\{ t_n n + \psi'(\delta_{eq}) \frac{\delta}{\delta_{eq}} ; t_n \leq 0 \text{ et } \delta_n \geq 0 \text{ et } t_n \delta_n = 0 \right\}$$

Note:

Warning : The translation process used on this website is a "Machine Translation". It may be imprecise and inaccurate in whole or in part and is provided as a convenience.

Copyright 2019 EDF R&D - Licensed under the terms of the GNU FDL (<http://www.gnu.org/copyleft/fdl.html>)

- There exists a field for the cohesive force, where discontinuity is worthless: it is the criterion of starting represented Figure 3.2-a dependent on nonthe derivability of Π in $\delta=0$. The form of the field depends on the expression on δ_{eq} .
- The condition of Kuhn and Tucker, which appears in - makes it possible to describe the conditions of contact (connects red Figure 3.2-a). In this case, t_n is negative, and corresponds to a compression whose value is not defined by the cohesive law.
- There exists a jump between the return to zero with worthless constraint (connects green) and the damage (connects blue), the cohesive force is thus not continuous compared to the jump of displacement.
- In the case of a pure mode I or of a mode of pure shearing, the answers of the cohesive law are those represented on Figure 3.2-a . The maximum values in traction and shearing are equal because of the choice of the standard.

3.3 Digital integration

According to, the digital integration of the cohesive law amounts calculating δ_g for values given of $[[u_g]]$ and of λ_g , and this for each point of Gauss (one omits now the index g). In fact, is a characterization of the following minimum:

$$\min_{\delta \in \mathbb{R}^3} \left[\lambda \cdot ([[u]] - \delta) + \frac{r}{2} ([[u]] - \delta)^2 + \Pi(\delta, \kappa) \right] \Leftrightarrow \lambda + r[[u]] - r\delta \in \partial \Pi(\delta, \kappa)$$

Moreover, evolution of the internal variable κ (see) must be taken into account. A temporal discretization is then necessary, consider a series of moments $t^0 < t^1 < \dots < t^n$ and corresponding quantities λ^n , $[[u^n]]$, δ^n and κ^n . At the time of the resolution, the iterative process is divided into two parts:

$$\delta^n = \operatorname{argmin}_{\delta \in \mathbb{R}^3} \left[\lambda^n \cdot ([[u^n]] - \delta) + \frac{r}{2} ([[u^n]] - \delta)^2 + \Pi(\delta, \kappa^{n-1}) \right]$$

$$\kappa^n = \max(\kappa^{n-1}, \delta_{eq}^n)$$

The second part is commonplace, minimization thus amounts solving the first with $\kappa = \kappa^{n-1}$ known parameter. A graphic interpretation of differential inclusion is provided on Figure 3.3-a (pure mode I without discharge): the solution corresponds to the intersection of the linear function $\delta \rightarrow \lambda + r[[u]] - r\delta$ (with a negative slope given by the coefficient of penalty r) with the graph $\partial \Pi(\delta, \kappa^{n-1})$.

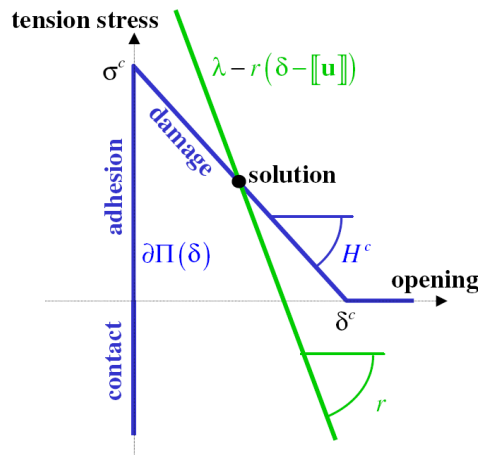


Figure 3.3-a : Solution of the integration of the behavior.

So that integration is robust, it is necessary that the function between hooks in that is to say strictly convex compared to δ (i.e that the minimum is single). While introducing H_c , the softening module of the cohesive law, one displays a sufficient condition to satisfy this condition (see 5 for more details):

$$r > \max_{x \geq 0} |\psi''(x)| = \frac{\sigma^c}{\delta^c} = H^c$$

Notice :

$r = 100 \times H^c$ is a value recommended to the user of Code_Aster.

It is supposed now that the condition is filled, moreover the function between hooks in is semi-continuous in a lower position, which guarantees the existence and the unicity of the minimum.

Now let us detail the digital integration of the law, i.e. the resolution of according to $\tau = \lambda + r[[u]]$. Taking into account the existence and unicity of the solution, it is interesting to use differential inclusion and the writing of the under-differential provided by with. The four cases thus are found:

- si $\kappa = 0$ et $\|\tau\|_+ \leq \sigma^c = \psi'(0)$: perfect adherence
 $\delta = 0$

- si $\kappa > 0$ et $\|\tau\|_+ < r\kappa$: return to zero with worthless constraint
$$\delta = \frac{\langle \tau \rangle_+}{r}$$

- si $\kappa > 0$ et $r\kappa \leq \|\tau\|_+ \leq r\kappa + \psi'(\kappa)$: vertical discharge
$$\delta = \kappa \frac{\langle \tau \rangle_+}{\|\tau\|_+}$$

- si $r\kappa + \psi'(\kappa) < \|\tau\|_+$: damage
$$\delta = \delta_{eq} \frac{\langle \tau \rangle_+}{\|\tau\|_+} ; \delta_{eq} \text{ solution de } \psi'(\delta_{eq}) + r\delta_{eq} = \|\tau\|_+$$

Notice :

| distinction $\kappa=0$ or is not necessary since seems a typical case of.

To conclude, the various modes of the cohesive law correspond to the solutions δ provided by -. These last are provided according to $\tau = \lambda + r[[u]]$. No digital method is necessary, indeed, the only equation to be solved (in) is linear per pieces.

4 Conclusion

A model finite element of interface, is proposed in order to model the evolution of cohesive cracks along a preset way. This last is compatible with the use of finite elements voluminal classics. Its unknown factors are nodal displacements on the lips of the cohesive crack as well as the nodal multipliers of Lagrange, corresponding to the surface density of the cohesive forces. The Lagrangian one of the problem is increased, that makes it possible to ensure a condition of convexity (via the parameter of penalization) which guarantees the unicity of the solution during the local integration of the law.

This approach presents however the following limits and disadvantages:

- The potential trajectories of the crack must be applied a priori.
- Additional degrees of freedom, correspond to the cohesive forces, are introduced. However their number remains relatively low since they are limited to the potential trajectories of the crack.
- The introduction of multipliers of Lagrange leads to a mixed formulation: the resolution of the problem thus returns to a search for point saddles and more to that of a minimum as it was the case in the initial energy formulation 5.
- It is necessary to increase the Lagrangian one to have a property of local convexity. That implies the introduction of a parameter of penalization, without influence on the continuous problem, but which could affect the results of the discretized problem. However, digital examples in 5 show that this sensitivity remains low and disappears with refinement from the grid.
- The local integration of the cohesive law rests on the calculation of discontinuities of displacement starting from the cohesive forces. An opposite approach is in general adopted in the literature for the elements of interface.

However a certain number of interesting properties emerge:

- No regularization of the cohesive law is necessary, in particular with regard to initial adherence or the condition of contact.
- The choice of a quadratic discretization for displacements and linear for the multipliers of Lagrange makes it possible to satisfy condition LBB. The latter makes it possible to ensure the convergence of the solution with the refinement of the grid in terms of displacements and cohesive forces (see digital example in 5).
- The rate of convergence which one would obtain without interface is not disturbed by the presence of the elements of interface (see 5).
- The search for point saddles leads to a symmetrical tangent matrix.
- This model of interface is compatible with the usual algorithms of resolution of *Code_Aster* such as the method Newton, linear research or the piloting of the loading. This is illustrated by calculations 2D and 3D in 5, thus showing the robustness and the reliability of such a model.

5 Bibliography

- [1] Bourdin B., Frankfurt G.A., Marigo J. - J. (2000) Numerical experiments in revisited brittle fracture. *J. Mech. Phys. Solids* **48** (4), 797-826.
- [2] Charlotte Mr., Laverne J., Marigo J. - J. (2006) Initiation of aces with cohesive force models: variational approach has. *European Newspaper of Mechanics A/Solids* **25** , 649-669.
- [3] Clarke F.H. Optimization and not smooth analysis. *Classics in applied mathematics* **5** , SIAM, 1990.
- [4] Del Piero G., Truskinovsky L. (2001) Macro and micro cracking in one dimensional elasticity. *Int. J. Solids Struct.* **38** , 1135-1148.
- [5] Fort Mr., Glowinski R. Augmented lagrangian methods: application to the numerical solution of boundary-been worth problems. *Studies in mathematics and its applications* **15** , North-Holland, 1983.
- [6] Frankfurt G., Marigo J. - J. (1998) Revisiting brittle fracture ace year energy minimization problem. *J. Mech. Phys. Solids* **46** (8), 1319-1342.
- [7] Fraternali F. (2007) Free discontinuity finite element models in two-dimensions for in-plane ace problems. *Theoretical and Applied Fractures Mechanics* **47** , 274-282.
- [8] Laverne J. Manual of reference of *Code_Aster* R7.02.11: Laws of behavior cohesive CZM_XXX_XXX and piloting of the loading.
- [9] Lorentz E., A mixed interface finite element for cohesive zone models, *Comput. Methods Appl. Mech. Engrg.* 198 (2008), 302-317.
- [10] Moes NR., Dolbow J., Belytschko T. (1999) A finite element method for ace growth without remeshing. *Int. J. Num. Meth. Engng.* **46** , 131-150.
- [11] Heel C., Curnier A. (2003) A model of adhesion coupled to contact and friction. *Eur. J. Mech. A/Solids* **22** (4), 545-565.

6 Description of the versions of the document

Index Doc.	Version Aster	Author (S) or contributor (S), organization	Description of the modifications
With	9.4	J.Laverne EDF/R & D /AMA E.Lorentz EDF/R & D /SINETICS	Initial text
	11.3	Mr. David EDF/R & D /AMA	Modification concerning the number of points used for the discretization of the jump